

# Structural, Morphological and Impedance Spectroscopic Analyses of Nano $\text{Li}(\text{Li}_{0.05}\text{Ni}_{0.4}\text{Co}_{0.3}\text{Mn}_{0.25})\text{O}_2$ Cathode Material Prepared by Sol-Gel Method

A. Nicholson<sup>1</sup>, S. Thanikaikarasan<sup>1</sup>, Pratap Kollu<sup>2</sup>, P.J. Sebastian<sup>3,†</sup>, T.Mahalingam<sup>4</sup> and X.Sahaya Shajan<sup>1,\*</sup>

<sup>1</sup>Centre for Scientific and Applied Research, PSN College of Engineering and Technology, Tirunelveli-627 152, Tamil Nadu, India.

<sup>2</sup>DST-INSPIRE Faculty, Department of Metallurgical Engineering and Materials Science, Indian Institute of Technology, Mumbai-400076, Tamil Nadu, India.

<sup>3</sup>IER-UNAM, 62580, Temixco, Morelos, Mexico

<sup>4</sup>Department of Electrical and Computer Engineering, College of Information Technology, Ajou University, Suwon 443 749, Republic of Korea.

Received: January 25, 2014, Accepted: July 14, 2014, Available online: October 03, 2014

**Abstract:** In the present work, layered lithium rich  $\text{Li}(\text{Li}_{0.05}\text{Ni}_{0.4}\text{Co}_{0.3}\text{Mn}_{0.25})\text{O}_2$  cathode materials were synthesized and its structural and electrical studies were analyzed. Layered  $\text{Li}(\text{Li}_{0.05}\text{Ni}_{0.4}\text{Co}_{0.3}\text{Mn}_{0.25})\text{O}_2$  cathode material was prepared by sol-gel technique using citric acid as chelating agent. The prepared sample was characterized by X-ray diffraction, SEM-EDS studies. The crystallite size of the  $\text{Li}(\text{Li}_{0.05}\text{Ni}_{0.4}\text{Co}_{0.3}\text{Mn}_{0.25})\text{O}_2$  cathode material was about 57 nm in which the diffusion path of lithium ion is effectively possible. The completion behavior of prepared cathode material was analyzed by FT-IR spectroscopy. The electrical properties of the prepared  $\text{Li}(\text{Li}_{0.05}\text{Ni}_{0.4}\text{Co}_{0.3}\text{Mn}_{0.25})\text{O}_2$  cathode material was studied by impedance and dielectric spectral analyzes. The maximum ionic conductivity of  $\text{Li}(\text{Li}_{0.05}\text{Ni}_{0.4}\text{Co}_{0.3}\text{Mn}_{0.25})\text{O}_2$  was found to be in the order of  $10^{-3.4}$  S/cm. The dielectric analysis of cathode material confirms the non-Debye type behavior.

**Keywords:** Sol-gel synthesis, nanoparticles, lithium batteries, ionic conductivity, dielectric properties.

## 1. INTRODUCTION

Lithium ion batteries (LIBs) are widely used in appliances such as cellular phones, digital cameras, laptops etc., due to their excellent properties such as high specific energy etc. A cathode material with less toxicity and more safety is in demand for cost effective LIBs [1]. Olivine phased cathode materials and layered cathode materials were in the limelight for lithium ion batteries for the past two decades [2]. Lithium cobalt dioxide was adopted as cathode material in commercial LIBs, because of its easy preparation, high electrical conductivity, high specific energy and stable discharge capacity. On the other hand, its low thermal stability and high cost are main obstacles to its application in large sized cells for hybrid-electric vehicles. Layer structured  $\text{LiNiO}_2$  and spinel structured  $\text{LiMnO}_2$  have been investigated as alternatives to  $\text{LiCoO}_2$ . In this regard, the reports on lithium-nickel-manganese-cobalt oxides

(LNMCOs) are having a greater fascination towards them [3]. Intensive research has been done on  $\text{LiNi}_{1/3}\text{Co}_{1/3}\text{Mn}_{1/3}\text{O}_2$  by Ohzuku and co-workers [4]. Following that, various stoichiometric ratios of LNMCO were studied. In addition, the surface modification and effect of dopants were under study. Amongst them the lithium rich LNMCO is in focus [5, 6]. Among the various synthetic routes [7-10] (such as co precipitation method, combustion method, solid state reaction method), sol gel method is observed as promising candidate for the synthesis of cathode materials. It is due to this reason that the cathode material prepared by this method possesses uniform particle size and good stoichiometry [11]. Moreover, the cathode materials considered in the present study can be synthesized with typical rhombohedral structure and can show monotonous charge-discharge behavior. Generally, the substitution of cobalt for nickel resulted in improved structural and electrochemical properties for the compound [12]. In this study, the compound  $\text{Li}(\text{Li}_{0.05}\text{Ni}_{0.4}\text{Co}_{0.3}\text{Mn}_{0.25})\text{O}_2$  was prepared by sol-gel method with citric acid as chelating agent. The chelating agent like

To whom correspondence should be addressed:  
Email: \*shajan89@gmail.com, †sjp@ier.unam.mx

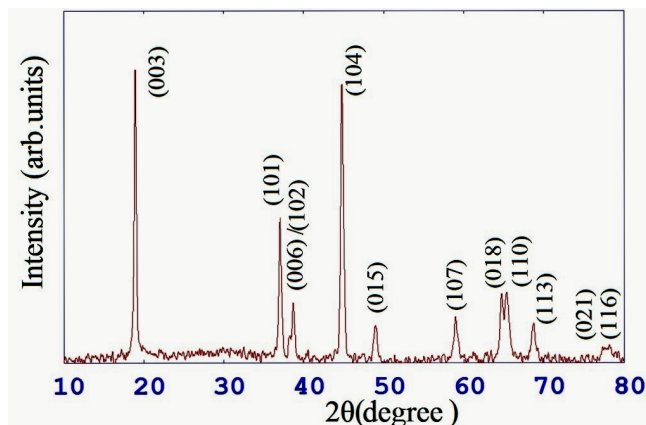


Figure 1. XRD pattern of  $\text{Li}(\text{Li}_{0.05}\text{Ni}_{0.4}\text{Co}_{0.3}\text{Mn}_{0.25})\text{O}_2$ .

citric acid acts on nitrate ions to decompose it and the heat evolved from the decomposition of nitrate is utilized to decompose the remaining organic constituents [13]. In this paper, the structural, morphological and electrochemical properties of  $\text{Li}(\text{Li}_{0.05}\text{Ni}_{0.4}\text{Co}_{0.3}\text{Mn}_{0.25})\text{O}_2$  cathode material synthesized by sol-gel method using citric acid as chelating agent were analyzed.

## 2. EXPERIMENTAL DETAILS

The precursor materials used are lithium nitrate ( $\text{LiNO}_3$ ) (Merck), manganese nitrate  $\text{Mn}(\text{NO}_3)_2 \cdot 6\text{H}_2\text{O}$  (Merck), nickel nitrate  $(\text{Ni}(\text{NO}_3)_2 \cdot 6\text{H}_2\text{O})$  (Merck) and cobalt nitrate  $\text{Co}(\text{NO}_3)_2 \cdot 6\text{H}_2\text{O}$  (Merck), citric acid ( $\text{C}_6\text{H}_8\text{O}_7$ ) (Merck). The cathode material  $\text{Li}(\text{Li}_{0.05}\text{Ni}_{0.4}\text{Co}_{0.3}\text{Mn}_{0.25})\text{O}_2$  was prepared by sol-gel method. The precursor materials were dissolved in distilled water and stirred for 7 hrs. Citric acid is added drop wise to the solution as a chelating agent. Ammonium hydroxide solution was added to the solution to maintain the pH between 6 and 7. The solution was heated to  $80^\circ\text{C}$  under continuous stirring to form a gel. The gel was preheated to  $500^\circ\text{C}$  for 4 hrs. Finally, the obtained powder was grounded well and calcined at  $850^\circ\text{C}$  for 15 hrs.

The powder X-ray diffraction (PANalytical-XPRT PRO, Netherlands) measurement using  $\text{CuK}\alpha$  radiation was employed to characterize the synthesized material. The morphological behavior and elemental analysis were done using SEM analyzer (JEOL-JSM.6400) with acceleration voltage of 5 kV. The FTIR spectra were recorded using JASCO FTIR/4100 spectrophotometer (Japan) in the region  $400\text{--}1100\text{ cm}^{-1}$  at room temperature with a signal resolution of  $8\text{ cm}^{-1}$ . Ionic conductivity measurements were carried out using impedance analyzer (Zahner IM6 Electrochemical Workstation (Germany)) in the frequency and temperature range of 100 mHz - 100 kHz and 303 K - 403 K respectively.

## 3. RESULTS AND DISCUSSION

### 3.1. Structural and Morphological Analyses

The XRD pattern of  $\text{Li}(\text{Li}_{0.05}\text{Ni}_{0.4}\text{Co}_{0.3}\text{Mn}_{0.25})\text{O}_2$  calcined at  $950^\circ\text{C}$  is shown in figure 1. The diffraction peaks observed is indexed based on the hexagonal  $\alpha\text{-NaFeO}_2$  structure with the space group of  $R\bar{3}m$ , which include the alternate layers of Li atom and  $\text{MO}_6$

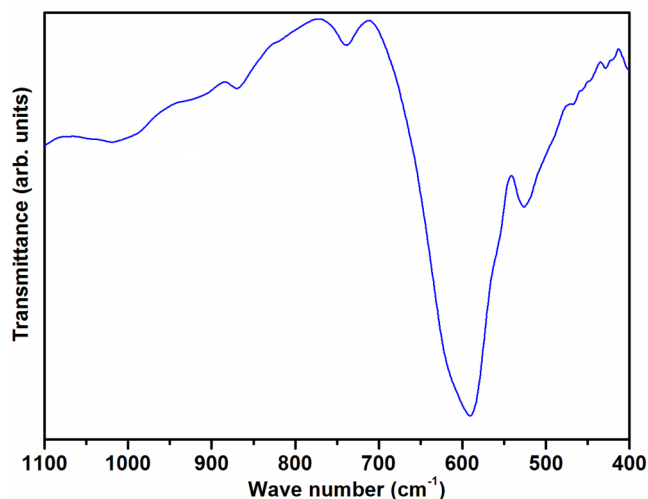


Figure 2. FTIR spectrum of  $\text{Li}(\text{Li}_{0.05}\text{Ni}_{0.4}\text{Co}_{0.3}\text{Mn}_{0.25})\text{O}_2$ .

octahedra ( $\text{M}=\text{Ni},\text{Co},\text{Mn}$ ) indicating pure phase layered crystal structure [14]. However, small diffraction peaks are seen between  $20^\circ$  to  $25^\circ$  ( $2\theta$ ), which shows the super lattice structure arising out of cation mixing of Li, Mn, Co and Ni atoms. This analogous behavior was reported by Lu et al and Kim et al [15-16], where they indicated the  $\text{LiMn}_2\text{O}_3$ . The peak splitting observed near  $38^\circ$  (006/012) and  $65^\circ$  (108/110) shows that the layered structure is well developed as reported by Kim *et al* [17]. The lattice constants were measured as  $a=2.8727\text{ \AA}$ ,  $c=14.0119\text{ \AA}$  and  $c/a$  ratio is 4.8776  $\text{\AA}$ , also the volume of the unit cell is  $V=100.137\text{ \AA}^3$ . The crystallite size can be estimated using Scherrer's formula given in eq. (1).

$$D = 0.9\lambda / \beta \cos\theta \quad (1)$$

where,  $\lambda$  is the wavelength of X-ray used, which is  $\text{CuK}\alpha$  radiation ( $\lambda=1.5406\text{ \AA}$ ), and  $\beta$  is the full width at half-maximum of the diffraction peak corresponding to  $2\theta$ . Using the above equation the sizes of the crystallites are found to be in the range of nanometer. The crystallite size is measured by taking the average of three main line widths, which are obtained from the XRD patterns. The crystallite size calculated using the Debye Scherrer formula is about 57 nm.

The vibrational spectrum in the range of  $400\text{--}1100\text{ cm}^{-1}$  for the synthesized LNMCO material is illustrated in figure 2. The very intense peak at  $600\text{ cm}^{-1}$  assigns to O-M-O bending modes and this may mask the characteristic peak of asymmetric M-O stretch, which is actually found at  $660\text{ cm}^{-1}$  ( $\text{M}=\text{Ni}/\text{Co}/\text{Mn}$ ). The significant peak obtained at  $545\text{ cm}^{-1}$  may be attributed to Li-O stretch which suggests the presence of lithium in the material. Furthermore, the less intense peaks observed at  $400$  and  $420\text{ cm}^{-1}$  could be allocated to weak inter-metallic interaction between any two metals present in the material. Besides, a band at  $271\text{ cm}^{-1}$  is also expected but it is not found in the achieved spectra because such lower region is not covered in the present study [9]. The surface morphology of  $\text{Li}(\text{Li}_{0.05}\text{Ni}_{0.4}\text{Co}_{0.3}\text{Mn}_{0.25})\text{O}_2$  was explored and identified by scanning electron microscopy. SEM image of  $\text{Li}(\text{Li}_{0.05}\text{Ni}_{0.4}\text{Co}_{0.3}\text{Mn}_{0.25})\text{O}_2$  is presented in figure 3. The image shows that particles are found to be agglomerated with spherulite

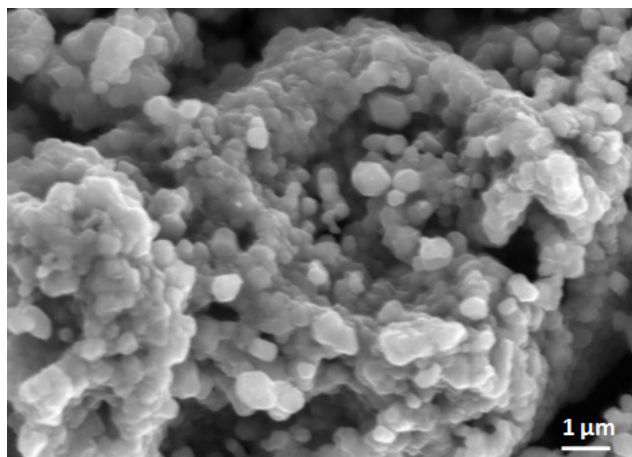


Figure 3. Scanning electron micrograph of  $\text{Li}(\text{Li}_{0.05}\text{Ni}_{0.4}\text{Co}_{0.3}\text{Mn}_{0.25})\text{O}_2$ .

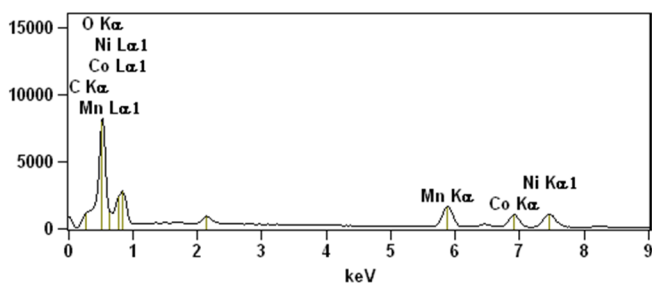


Figure 4. Energy Dispersive Spectrum of  $\text{Li}(\text{Li}_{0.05}\text{Ni}_{0.4}\text{Co}_{0.3}\text{Mn}_{0.25})\text{O}_2$ .

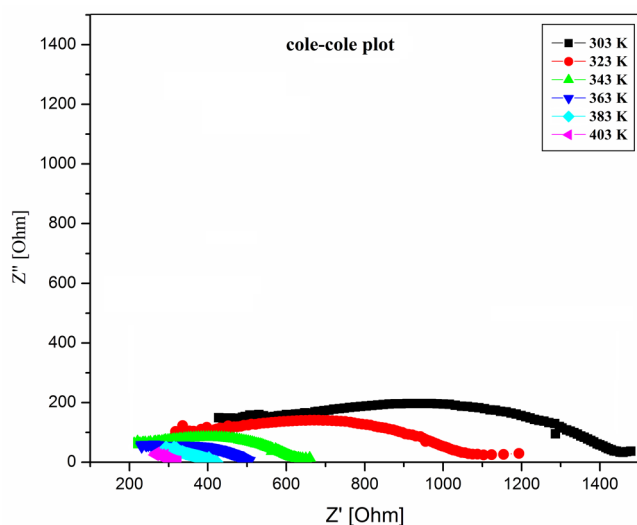


Figure 5. Cole-Cole impedance plot of  $\text{Li}(\text{Li}_{0.05}\text{Ni}_{0.4}\text{Co}_{0.3}\text{Mn}_{0.25})\text{O}_2$  at different temperatures.

morphology. Moreover the grains are found to be formed in different sizes mostly in the range of 200-250 nm. Figure 4 shows the

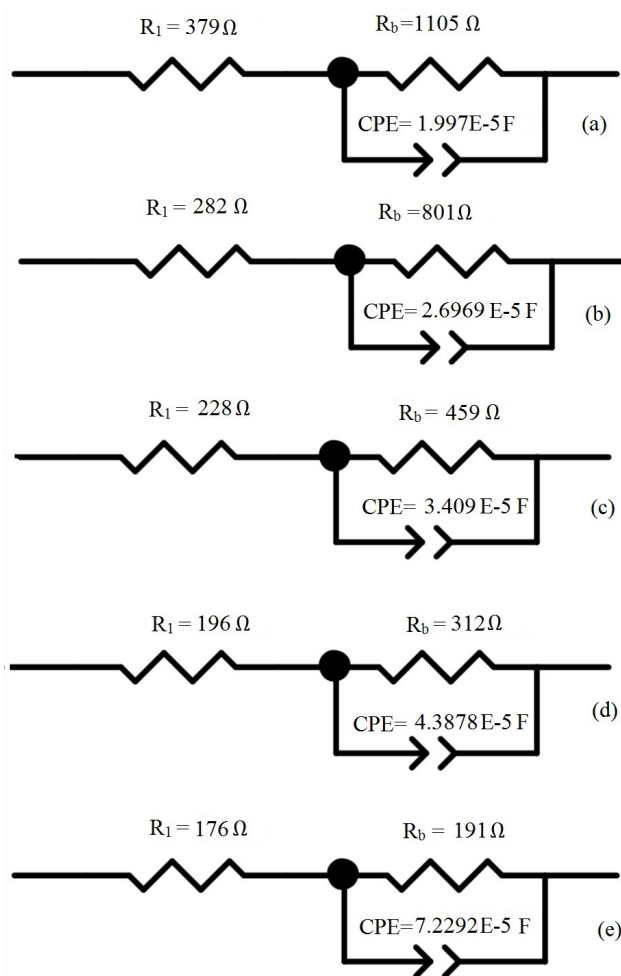


Figure 6. Equivalent circuit of  $\text{Li}(\text{Li}_{0.05}\text{Ni}_{0.4}\text{Co}_{0.3}\text{Mn}_{0.25})\text{O}_2$  material at (a) 403 (b) 423 (c) 443 (d) 463 (e) 483 K.

EDX spectrum of the compound. The presence of emission lines of Ni, Mn, Co and O in the investigated energy range indicates the formation of LNMCO compound. The absence of Li ion in the spectra indicates the low atomic ratio of Li.

### 3.2. Electrochemical Impedance Analysis

The ionic conductivity of the prepared  $\text{Li}(\text{Li}_{0.05}\text{Ni}_{0.4}\text{Co}_{0.3}\text{Mn}_{0.25})\text{O}_2$  was calculated by means of the following equation (2).

$$\sigma = \frac{t}{R_b A} \quad (2)$$

where,  $t$  and  $A$  are the thickness and area of the  $\text{Li}(\text{Li}_{0.05}\text{Ni}_{0.4}\text{Co}_{0.3}\text{Mn}_{0.25})\text{O}_2$  in contact with the gold blocking electrodes respectively. Thickness of the  $\text{Li}(\text{Li}_{0.05}\text{Ni}_{0.4}\text{Co}_{0.3}\text{Mn}_{0.25})\text{O}_2$  was measured by means of micrometer screw gauge.  $R_b$  represents the bulk resistance, which was obtained from extrapolation of semi-circular region to higher frequencies. Figure 5 represents the cole-cole impedance plot for  $\text{Li}(\text{Li}_{0.05}\text{Ni}_{0.4}\text{Co}_{0.3}\text{Mn}_{0.25})\text{O}_2$ . It is inferred from the plot that at high frequencies a compressed semicircle was

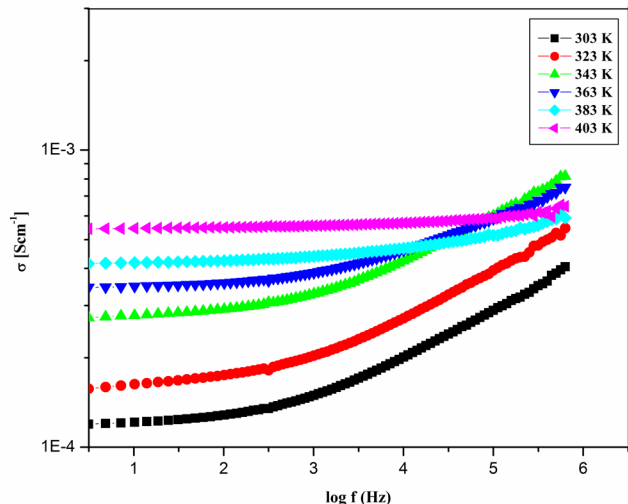


Figure 7. Ionic conductivity vs temperature for  $\text{Li}(\text{Li}_{0.05}\text{Ni}_{0.4}\text{Co}_{0.3}\text{Mn}_{0.25})\text{O}_2$ .

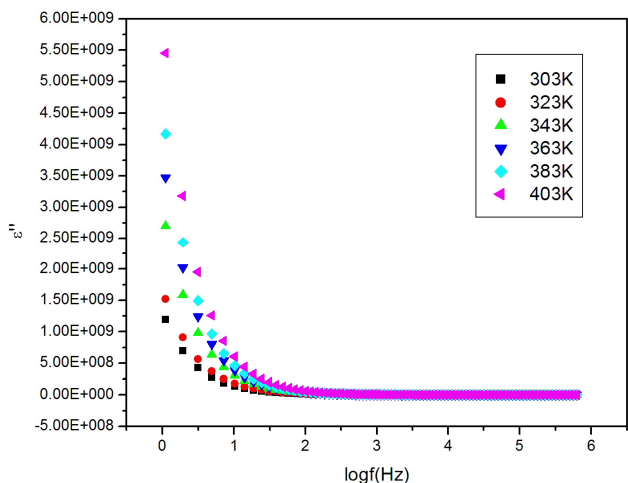


Figure 8. Arrhenius plot of  $\text{Li}(\text{Li}_{0.05}\text{Ni}_{0.4}\text{Co}_{0.3}\text{Mn}_{0.25})\text{O}_2$ .

obtained. This may due to the distribution of relaxation times. Figure 6 shows the equivalent circuit of  $\text{Li}(\text{Li}_{0.05}\text{Ni}_{0.4}\text{Co}_{0.3}\text{Mn}_{0.25})\text{O}_2$  at different temperatures. The equivalent circuit represents the parallel combination of resistance and capacitance. The bulk resistance  $R_b$  value decreased with increase in temperature. The increase in capacitance with respect to the temperature shows the accumulation of charge carriers at the electrode surface. At low frequency, an inclined spike was obtained. The ionic conductivity as a function of temperature for  $\text{Li}(\text{Li}_{0.05}\text{Ni}_{0.4}\text{Co}_{0.3}\text{Mn}_{0.25})\text{O}_2$  is shown in figure 7. It is observed from figure 6 that ionic conductivity increases with increase in temperature. The ionic conductivity of  $\text{Li}(\text{Li}_{0.05}\text{Ni}_{0.4}\text{Co}_{0.3}\text{Mn}_{0.25})\text{O}_2$  obeys Arrhenius law of conduction mechanism.

$$\sigma = \sigma_0 A e^{-E_a/KT} \quad (3)$$

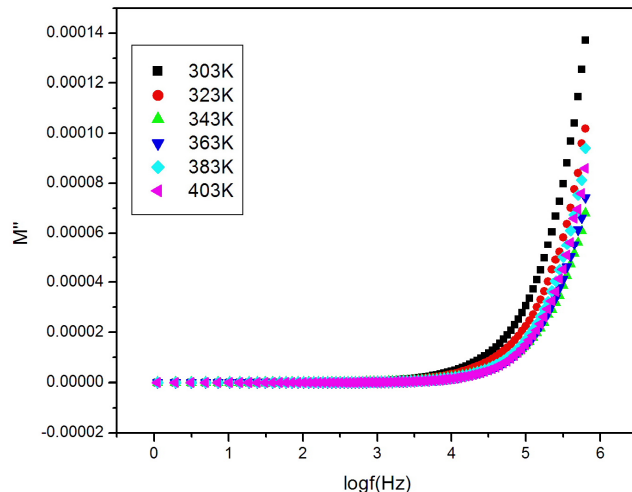


Figure 9. Logarithm of  $\omega$  versus dielectric loss  $\epsilon''$  at different temperatures.

where, A and K are constants.  $E_a$  is the activation energy of the sample. It was calculated from the slope of the linear fit of Arrhenius plot and its value is found to be 0.16 eV (figure 8). Further, the increase in ionic conductivity is also due to the availability of conducting ions in the material [18, 19]. It is inferred from figure 8 that the maximum ionic conductivity of prepared sample is found to be in the order of  $10^{-3.4}$  S/cm. This result is in accordance with the earlier report [20].

### 3.3. Dielectric Spectra Analysis

Study of the dielectric process is an important tool for valuable information about conduction process. The dielectric property indicates the amount of charge that can be stored by a material and it can be used as an indicator to prove the increase in ionic conductivity is due to increase in charge carriers. A wide frequency dielectric relaxation spectroscopy is a tool to study the relaxation of dipoles. The complex permittivity  $\epsilon^*$  or dielectric constant of a system is evaluated by means of following expression,

$$\epsilon^* = \epsilon' - j\epsilon'' \quad (4)$$

where,  $\epsilon'$  is the real part of dielectric constant and  $\epsilon''$  is the imaginary part of dielectric constants

$$\epsilon' = \frac{cd}{\epsilon_0 A} \quad (5)$$

$$\epsilon'' = \frac{\sigma'}{\omega \epsilon_0} \quad (6)$$

where,  $\sigma'$  is the real part of conductivity (S/cm), C is the parallel capacitance (F); d (cm) and A ( $\text{cm}^2$ ) are thickness and area of the pelletized  $\text{Li}(\text{Li}_{0.05}\text{Ni}_{0.4}\text{Co}_{0.3}\text{Mn}_{0.25})\text{O}_2$  respectively,  $\omega$  the angular frequency and  $\epsilon_0$  is the permittivity of free space which is equal to  $8.856 \times 10^{-14}$  F/cm. Figure 9 represents the variation of  $\epsilon''$  as a function of log frequency for  $\text{Li}(\text{Li}_{0.05}\text{Ni}_{0.4}\text{Co}_{0.3}\text{Mn}_{0.25})\text{O}_2$  at different

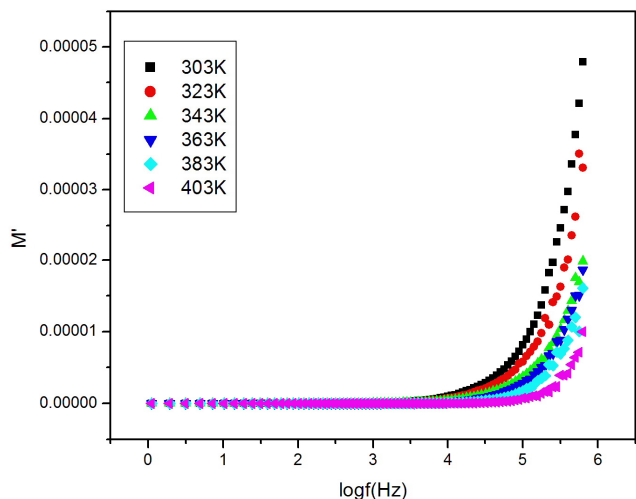


Figure 10. Logarithm of  $\omega$  versus real part of modulus of  $\text{Li}(\text{Li}_{0.05}\text{Ni}_{0.4}\text{Co}_{0.3}\text{Mn}_{0.25})\text{O}_2$  at different temperatures.

temperature. The dispersion of dielectric constant is high at low frequency for all temperatures and this may be attributed to the formation of space charge region at the electrode interface, which is commonly known as  $\omega^{(n-1)}$  variation or non-Debye nature of the behavior, where the space charge regions with respect to the frequency are explained in terms of ion diffusion [21]. At higher frequencies the change in the direction of the electric field lines is too fast to be followed by the charged ions and hence the dielectric constant decreases. From figure 9 it is identified that the dielectric constant increases with increase in temperature.

### 3.4. Modulus Spectra Analysis

The modulus spectra mainly reflect the bulk properties of the sample. Electric modulus relaxation studies were carried out between 303K and 403K in the complex modulus  $M^*$  formalism. The complex modulus is given by the inverse of the complex dielectric permittivity

$$M^* = \frac{1}{\epsilon^*} = M' + M'' \quad (7)$$

Variation of real ( $M'$ ) and imaginary ( $M''$ ) parts of the electric modulus as a functions of frequency at various temperatures are shown in figures 10 and 11. As the temperature increases, the peaks of  $M'$  and  $M''$  have decreased gradually due to plurality of relaxation mechanism. The values of  $M'$  and  $M''$  tend to be zero in the vicinity at lower frequencies which proposes that the electrode polarization at the interface is negligible at lower frequencies [22]. The presence of long straight line in the low frequency region confirms a large equivalent capacitance associated with the electrode interface. In the mean time the value of  $M''$  decreased slowly at higher temperature due to decrease in charge carrier density at the space accumulation region.

## 4. CONCLUSIONS

Sol-gel type lithium rich  $\text{Li}(\text{Li}_{0.05}\text{Ni}_{0.4}\text{Co}_{0.3}\text{Mn}_{0.25})\text{O}_2$  cathode

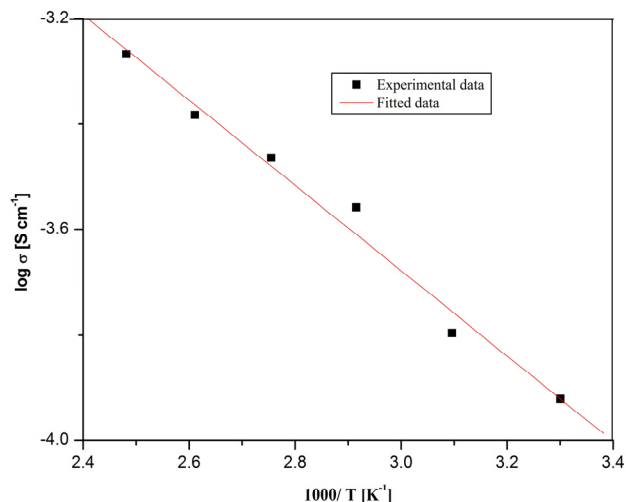


Figure 11. Logarithm of  $\omega$  versus real part of modulus of  $\text{Li}(\text{Li}_{0.05}\text{Ni}_{0.4}\text{Co}_{0.3}\text{Mn}_{0.25})\text{O}_2$  at different temperatures.

material in nano dimension was prepared using citric acid as chelating agent. The cathode material resembled the hexagonal  $\alpha$ - $\text{NaFeO}_2$  structure which was confirmed from XRD pattern. The presence of all the elements in the cathode material was pre-determined and was confirmed by EDS. The prepared material possessed an excellent electrical property, which was inferred from ionic conductivity analysis. The maximum ionic conductivity was found to be in the order of  $10^{-3.4}$  S/cm. The dielectric spectra analysis showed a non-Debye nature behavior of the material. The higher value of dielectric constant with increase in temperature represented the increase in polarizability in the material. This result strongly supports the results obtained in ionic conductivity analysis.

## REFERENCES

- [1] J.M. Tarascon, M. Armand, Nature, 414, 359 (2001).
- [2] J.W. Fergus, J. Power Sources, 195, 939 (2010).
- [3] N. Yabuuchi, T. Ohzuku, J. Power Sources, 119, 117 (2003).
- [4] Y. Koyama, I. Tanaka, H. Adachi, Y. Makimura, T. Ohzuku, J. Power Sources, 119, 644 (2003).
- [5] S.J. Shi, J.P. Tu, Y.Y. Tang, X.Y. Liu, Y.Q. Zhang, X.L. Wang, C.D. Gu, Electrochim. Acta, 88, 671 (2013).
- [6] Q. Liu, K. Du, H. Guo, Z.D. Peng, Yan-bing Cao, Guo-rong Hu, Electrochim. Acta, 90, 350 (2013).
- [7] L.J. Fu, H. Liu, C. Li, Y.P. Wu, E. Rahm, R. Holze, H.Q. Wu, Prog. Mater. Sci., 50, 881 (2005).
- [8] T.H. Cho, S.M. Park, M. Yoshio, T. Hirai, Y. Hideshima, J. Power Sources, 142, 306 (2005).
- [9] P. Suresh, S. Rodrigues, A.K. Shukla, H.N. Vasan, N. Muni-chandraiah, Solid State Ionics, 176, 281 (2005).
- [10] S.H. Kang, I. Belharouak, Y.K. Sun, K. Amine, J. Power Sources, 146, 650 (2005).
- [11] K.S. Park, M.H. Cho, S.J. Jin, K.S. Nahm, Y.S. Hong, Solid State Ionics, 171, 141 (2004).

- [12]A. Rougier, I. Saadoune, P. Gravereau, P. Willmann, C. Delmas, *Solid State Ionics*, 90, 83 (1996).
- [13]B.J. Hwang, R. Santhanam, D.G. Liu, *J. Power Sources*, 443, 97 (2001).
- [14]S.K. Jeong, C.H. Song, K.S. Nahm, A.M. Stephan, *Electrochim. Acta*, 52, 885 (2006).
- [15]Z. Lu, J.R. Dan, *J. Electrochem. Soc.*, 149, A815 (2002).
- [16]J.H. Kim, C.W. Park, Y.K. Sun, *Solid State Ionics*, 164, 43 (2003).
- [17]H.S. Kim, M. Kong, K. Kim, I.J. Kim, H.B. Gu, *J. Power Sources*, 171, 917 (2007).
- [18]K. Karuppasamy, C. Vijil Vani, R. Antony, S. Balakumar, X. Sahaya Shajan, *Polym. Bull.*, 70, 2531 (2013).
- [19]K. Karuppasamy, C. Vijil Vani, A. Nicholson, S. Balakumar, X. Sahaya Shajan, *AIP Conf. Proc.*, 1536, 45 (2013).
- [20]M.G.S.R. Thomas, P.G. Bruce, J.B. Goodenough, *Solid State Ionics*, 18&19, 794 (1986).
- [21]F.S. Howell, R.A. Bose, P.B. Macedo, C.T. Moynihan, *J. Phys. Chem.*, 78, 639 (1974).
- [22]K.S. Rao, D.M. Prasad, P.M. Krishna, B. Tilak, K.C. Varadara-julu, *Mater. Sci. Eng. B.*, 133, 141 (2006).